

Mathematical modeling of thin layer drying of green plantain (*Musa paradisiaca* L.) peel

¹*Faneite, A. M., ²Rincón, A., ³Ferrer, A., ⁴Angós, I. and ⁵Arguello, G.

¹Laboratorio de Ingeniería Química “Prof. Ydelfonso Arrieta”, Escuela de Ingeniería Química, Facultad de Ingeniería, Universidad del Zulia. Maracaibo, Venezuela

²Escuela de Ingeniería Química, Facultad de Ingeniería, Universidad Rafael Urdaneta. Maracaibo, Venezuela

³Instituto Zuliano de Investigaciones Tecnológicas. Km 15 vía La Cañada de Urdaneta, Venezuela

⁴Facultad de Ciencia e Ingeniería en Alimentos, Universidad Técnica de Ambato, Campus Huachi. Ambato, Ecuador

⁵Instituto Nacional de Investigaciones Agrícolas (INIA). Trujillo, Venezuela

Article history

Received: 27 May 2015

Received in revised form:
29 January 2016

Accepted: 9 February 2016

Abstract

In this work green plantain peel was characterized in terms of moisture, and dry basis hemicellulose (HC), cellulose, lignin, crude fiber (CB), crude protein (CP), ether extract (EE), starch, nitrogen free extract (NFE), total digestible nutrients (TDN) and ash. According to the high proportion found of hydrophilic components (carbohydrates) and water (76.15 % and 87.62 % respectively) a slow drying period was determined. Drying kinetics of peels at 60, 70, 80, 90, 100 and 110 °C was studied. Isothermal drying curves for green plantain peels showed a monotonic decreasing of moisture content in the whole range of temperatures studied, until a point where the changes of the moisture content were very little in function of time, indicating that the transition state of dynamic pseudo-equilibrium (TSDPE) was reached. Best fit was found when modified Henderson-Pabis model was used. Desorption, drying rate, and effective diffusivity curves showed a non fickian process, a drying period of decreasing rate with internal control, and a concentration-dependence diffusion, respectively.

Keywords

Lignocellulosic materials
Equilibrium moisture
Regular regime
Anomalous diffusion
Activation energy

© All Rights Reserved

Introduction

Plantain is one of the most relevant crops in the world in value ($10 \cdot 10^7$ T/year) (FAO, 2013). However, plantain peel has been traditionally considered as a low prized by-product (Chambron, 2000). Taking into account that plantain peel represent about 20 % of total weight of the fruit (Ly, 2004) more than $7 \cdot 10^6$ T of waste disposal are produced on a year basis. Management of plantain peels have become thus an environmental challenge due to its contaminant properties (Intriago and Paz, 2000).

Plantain peels doesn't play yet a relevant role at industrial scale but there are several promising processes to obtain ruminant feed and ethanol as final products (Mohapatra *et al.*, 2010). The latter is being studied in many countries as alternative sources of fuels due to the decreasing reserves of oil estimated in less than 50 years due to constant rising of consumption (OPEC, 2015).

Plantain peels has a high potential in ethanol production due to the high productivity of the crop (FAO, 2013) but its high moisture content up to 91

% (wet basis) make bulk storage and management not affordable unless a previous drying process be implemented (Monsalve *et al.*, 2006). Design and construction of drying facilities have to be started determining first its characteristic drying isotherms and mathematic models describing them.

The main objective of this work was to study the drying kinetics of green plantain peel, the use of a new rigorous statistical procedure to select the best empirical drying kinetics model, the analysis of the phenomenology implied in the water transport through the material using desorption and drying rate curves, and developing a new calculation method of the effective diffusivity, based on the regular regime method, and, finally, comparing this method against the traditional activation energy method.

Materials and Methods

Sampling

75 Hartón variety plantains were obtained in June 2011 in the “Santa Rosa” farm located in Pueblo Nuevo-El Chivo, in the south region of Lake

*Corresponding author.

Email: afaneite@fing.luz.edu.ve

Tel: +58-414-3689396

Maracaibo in the state of Zulia, Venezuela, with geographical coordinates 08°56'22" N, 71°37'47" W. Experimental schedule consisted in sampling 10% of the total cultivated surface, meaning 50.000 m² distributed in five plots of 100 x 100 m². From each plot five sample units of three plantains were obtained; four samples were collected at three meters from each corner of the plot and the fifth in the middle of the field. Standard fertilizing of this crop is 350-400 kg·ha⁻¹ N, 50 kg·ha⁻¹ P₂O₅, 600 kg·ha⁻¹ K₂O, 560 kg·ha⁻¹ CaO and 100 kg·ha⁻¹ MgO (Espinosa and Mite, 2002) having a harvest time of about nine months.

Characterization of plantain peeling

Initial moisture and starch content were determined according to venezuelan standards COVENIN 1156-79 (COVENIN, 1979) and 376-81 (COVENIN, 1981), respectively. Cellulose, HC and lignin content were determined by means of the Goering and Van Soest fractional method. Crude Protein (CP), Ethereal Extract (EE), Crude Fiber (CF) and ash was determined following the Weende method of proximate analysis (Garrett, 1974). Total Digestible Nutrients (TDN) were determined following Van Soest (1963) *in vitro* digestibility method, and Nitrogen Free Extract (NFE) was calculated by difference from total dried weight subtracting CP, EE, CF and ash. All determinations were done in triplicate.

Determination of drying kinetics at several temperatures

After harvesting whole green plantains were stored at 7 °C in sealed bags containing small pieces of lemon preventing ripening before processing (less than one week from harvest). Just before each experiment trial, green plantains were peeled and gently washed with water, being the fruit discarded. A thin layer of known thickness of plantain peels was made to cover all surface of the sample holder before being subjected to hot airstream at 60, 70, 80, 90, 100 or 110°C. Initial weighting interval was five minutes between 60 and 80 °C and three minutes between 90 and 110 °C. Drying was considered to be finished when constant weight (state of dynamic pseudo-equilibrium) was reached. Dried samples were transferred to a drying oven at 105 °C for 24 h and finally weighted. All determinations were done in triplicate.

Calculation method of experimental drying curves

Dry basis (d.b.) moisture content was calculated with equation 1:

$$X(t) = (m(t) - m_{final}) / m_{final} \quad \text{Eq. 1}$$

where: $X(t)$ is d.b. moisture content, $m(t)$ is mass weight over time (t), m_{final} is mass weight after oven drying. Moisture contents (d.b.) were expressed in terms of remaining moisture fraction ($Mr(t)$) with equation 4, and then plotted versus time.

Transition state of dynamic pseudo-equilibrium

The traditional form to express the moisture content in the studies of drying kinetics is the dry basis (d.b.) remaining moisture fraction (Mr), and Mr over time expressed as $Mr(t)$, can to see in equation 2.

$$Mr(t) = (X_{(t)} - X_e) / (X_0 - X_e) \quad \text{Eq. 2}$$

where $X_{(t)}$ is d.b. moisture content over time, X_0 is d.b. initial moisture content, and X_e is d.b. moisture content in the equilibrium state. X_e is normally eliminated of equation 2 due its value is very low, resulting equation 3.

$$Mr(t) = X_{(t)} / X_0 \quad \text{Eq. 3}$$

Figure 1 shows the drying of any material, in terms of equation 3 in function of the time, from $Mr(t) = 1$ to infinity. Drying beginning with monotonic decrease of the moisture content where many of the thin layer drying models, explain this behavior very efficiently, for many materials. In a moment of the drying process (t_{xdpe}), well below of the normal storage humidity (X_s/X_0 in the Figure 1, between 10 and 5 % in wet basis), the behavior changes abruptly to a very slow decrease of the moisture content that can be physically appreciated with changes in the weight of the sample in an order of 10⁻³ and 10⁻⁴ g, in the drying kinetics experiments. This condition could make think that the process has reached a stationary (equilibrium) state, but really it is a pseudo-equilibrium state. At the same temperature of the drying curve, the material can be for a long of time in this transition state between the kinetics processes, governed by external (air) and internal (material) transport phenomena, and the real equilibrium state where govern surface phenomena. Obviously, the equilibrium moisture (X_e/X_0) is very low compared with the dynamic pseudo-equilibrium moisture (X_{dpe}/X_0), and the time between these two point is very high ($t_{xdpe} - t_{xe}$). Being X_{dpe}/X_0 , the finish of the behavior explained by all the thin layer drying models, is logical that this point be the limit used in the equation of Mr . The term "dynamic" comes from the fact that the real equilibrium moisture content is determined by the "gravimetric static method" (Molnár, 2006), but the dynamic pseudo-equilibrium moisture

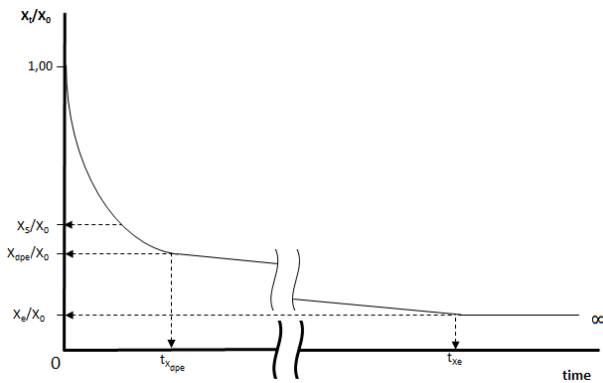


Figure 1. Illustrative figure of the monotonic decrease of the moisture content in the drying of any material (From $X_t/X_0=1$ to X_{dpe}/X_0), followed of the transition state of dynamic pseudo-equilibrium (TSDPE) (From X_{dpe}/X_0 to X_e/X_0), followed of the real equilibrium state (From X_e/X_0 to infinity)

content is found in a drying experiment where the air has a movement. Thus, using equation 4 is proposed, in order to avoid errors in the simulations and design of industrial dryers where drying times or output moistures can be underestimated or overestimated, respectively.

$$Mr(t) = (X_{(t)} - X_{dpe}) / (X_0 - X_{dpe}) \quad \text{Eq. 4}$$

Empirical modeling methodology using experimental data smoothing, ANOVA, and the criteria of trend, bias and randomness of the best model

Smoothed plots of Mr were calculated by means of polynomial fitting with the Excel® graphic tool “Trend line”. The resulting polynomial equations were used to re-calculate the drying curves (smoothed) but with a time interval (Δt) of 0.2 min. Parameters of the thin layer drying models evaluated, using the drying curves smoothed, were adjusted by means of least square method implemented with the Solver tool from Excel®.

Comparing the graphics of experimental drying curves against models, and the graphic of Mr Residuals, a first discard can to be done with these statistical criteria of visual inspection. The model discarded with the visual inspection, is the one who does not follow the behavior of the experimental drying curve, and which Mr residuals have some tendency and little randomness. Then, statistical criteria of analytical selection were calculated, in order to evaluate the models that were not discarded in the visual inspection. The Coefficient of Determination (R^2), was used as a measure of how well the model follows the “trend” of the experimental data; Mean biased error (MBE) and Mean Relative Deviation (MRD) were used as a measure of the equitable

distribution of the experimental points around the models (randomness); Root Mean Square Error (RMSE) and Ji Square (χ^2) were used as a measure of the “bias” of the models with respect to the experimental points. Finally ANOVA and LSD test at 95 % of significance was calculated by means of Statistix 8 software, putting the models as treatments and temperature as repetitions, for each statistical criteria of analytical selection.

Drying rate curves

Polynomic equations resulting of the smoothing of the experimental curves were derived with respect to time. Finally, $-dMr(t)/dt$ data versus $Mr(t)$ were plotted at full Mr range for each temperature.

Desorption curves

Desorption curves were calculated subtracting the mass of each drying point (mt) from the initial mass ($me = m_0 - m_{final}$) and dividing by the total mass of water removed (mt/me). Data of (mt/me) was plotted versus the square root of the time. The behavior of the curves was compared with the behavior of the different types of desorption defined by Rogers (Crank, 1975b).

Qualitative kinetic data analysis by means of a regular regime as an alternative procedure to activation energy method

Crank’s solution to the second Law of Fick (Crank, 1975a), is usually employed to describe the diffusional process of the water inside the material during drying, assuming that the diffusional coefficient is constant. When truncating in the first term the Crank’s solution to the second Fick Law (Crank, 1975a), equation 5 is obtained, offering a theoretical approximation to the description of the drying for the sample, in a plane geometric figure defunding in a transversal way to its thickness only for a face, where L is the thickness of the layer (m), t is time (s), and diffusional coefficient is substituted by the term $Deff$ which is the effective diffusivity (m^2/s).

$$Mr(t) = \frac{8}{\pi} \exp\left(-\frac{\pi^2 \cdot Deff \cdot t}{L^2}\right) \quad \text{Eq. 5}$$

$Deff$ is the first empirical modification introduced in this equation, and this implies that phenomena of transport of the water as capillarity, vapor diffusivity, and pressure, whose expressions have to be summative together with the liquid diffusivity are included inside the expression of the liquid diffusivity (Eq. 5) (Treybal, 1980). The second empirical modification is the adaptation of Eq. 5 to the fact that the first point of the drying curve, at

time equal to 0, has a value of 1. Normally, the pre-exponential factor $8/\pi$ is empirically substituted by 1, to adjust this truncated equation to the experimental data. This can be clearly seen in empirical thin-layer drying models. The supposition that the length of the layer (L) is also constant is something that needs to be evaluated for each material.

Lignocellulose is a material in which is very unlikely that a ficktian diffusivity of the water stays could be seen due to its internal sites with a complex structure, constituting mainly by hydrophilic polysaccharides as cellulose, hemicellulose and pectin, and that in turn, containing hydrophobic substances as lignin and waxes in it surface that act as anti-dehydration barriers. If the non-ficktian diffusivity is demonstrated when using the drying rate curves and desorption curves (Crank, 1975b), equation 5 shouldn't be used. However, effective diffusivity is usually reported constant for lignocellulosic materials where in a plot of $\ln Mr$ vs t , the slope is obliged to be linear.

On the other hand, when authors plot $\ln Deff$ vs $1/T$ (1/K), normally obtain a linear slope, equivalent to an Arrhenius expression that has an implicit energetic parameter known as activation energy (Ea). Come up to the calculation of Ea is equivalent to a "dead end" because there is no explanation of its meaning in the literature, nor its relationship with other thermodynamic properties of the biomass-water system, only limited in some cases to the comparison with the Ea of other materials, but without concluding theoretically in relation with the differences in the drying based in this parameter (Rao et al., 2014). Pre-exponential factor of the Arrhenius expression, designed by D_0 , is only reported without a theoretically explanation. Then, if these two terms, don't afford sufficient information for high quality modeling and don't give information about the phenomenology implicit in the drying process with respect, e. g. the ficktianity or the resistance of water desorption, a question arise: why do these parameters continue being calculated?

Taking into account that lignocellulosic materials are fibrous compounds with high content of hydrophilic carbohydrates, whose molecules bind intermolecularly, crystallizing or changing its crystallinity during drying (Weise, 1998), it is very probable that the diffusion coefficient is concentration-dependent. Plotting $Deff$ vs Mr ; calculated with equations 5 and 4, respectively, and verifying a potential behavior, demonstrates that $Deff$ is not constant, describing its behavior by means of equation 6.

$$Deff = (b + mT) \cdot Mr^n \quad \text{Eq. 6}$$

Table 1. Characterization of green plantain peels

Parameter	Percentage (%) ^a
Moisture	87.62
Hemicellulose	45.4
Cellulose	6.68
Lignin	2.93
Crude fiber	5.13
Crude protein	8.78
Fat	2.47
Starch	6.92
NFE	71.55
TDN	71.04
Ash	12.07

NFE. Nitrogen free extract. TDN Total digestible nutrients. ^(a)
Note: All data expressed in dry basis (d.b.) except moisture, expressed in wet basis (w.b.).

where, b , m and n are parameters of model, and T is temperature (K). Plotting in separate both terms of equation 6 ($b + mT$, and Mr^n), allows to obtain two graphics that can be proposed to analyze qualitatively drying data. The first term or 'velocity' denotes (in the graphic $b + mT$ vs T) which material is dried faster than others, and the second term or 'concentration' term denotes (in the graphic Mr^n vs Mr) the ficktianity of the drying without the need to compare with the drying of other materials. This Regular Regime Approach proposal is very close to the Method of Coumans (Adhikari et al., 2002) but much simpler, just looking an alternative tool to the energy activation method.

Effective diffusivity curves

Effective diffusivity ($Deff$) was calculated for each experimental point with the equation 5. $Deff$ was then plotted in function of Mr , calculated with equation 4. Once diffusivity was evaluated to have a potential behavior, regular regime model parameters were calculated.

Graphics of the regular regime approach

With the effective diffusivity curves, parameters of equation 6 were calculated using Solver of Excel[®]. The 'velocity' term of equation 6 ($b + mT$) was plotted in function of the temperature, and the 'concentration' term denotes (Mr^n) was plotted in function of Mr . Both terms were compared with other experimental drying data of similar lignocellulosic materials, available in the literature (Faneite et al., 2012).

Results and Discussion

Characterization of green plantain peeling

Characterization of green plantain peels is presented in Table 1. Wet basis moisture content

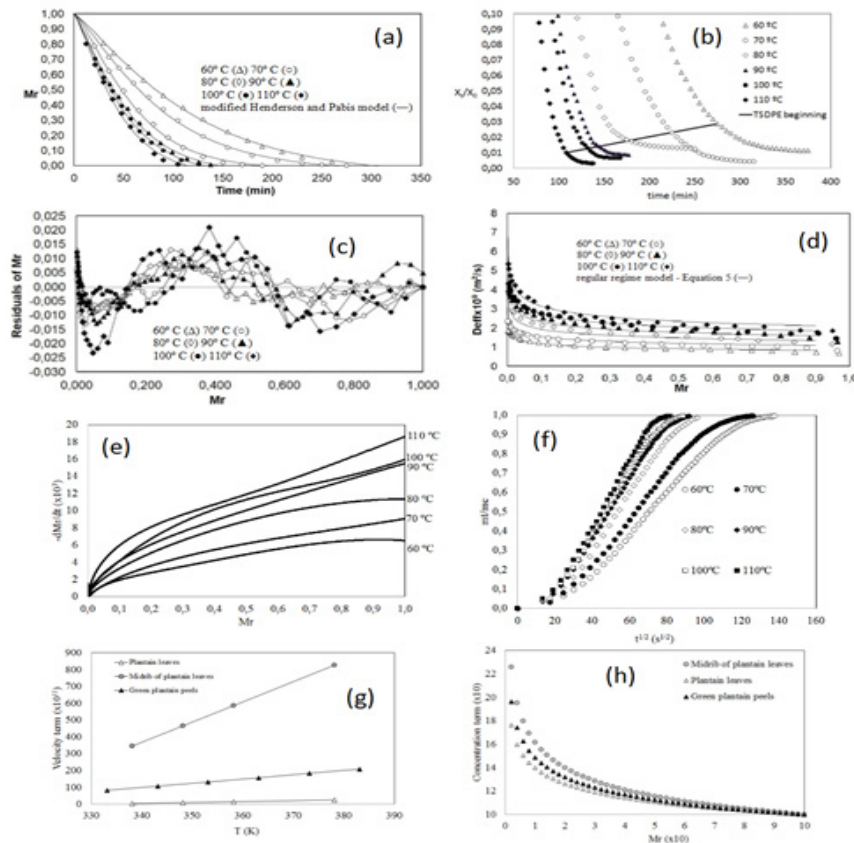


Figure 2. (a) Experimental drying kinetics data and the best model, (b) detail of the beginning of dynamic pseudo-equilibrium TSDPE, (c) residuals graphic of Mr (d) graphic of effective diffusivity, (e) drying rate curves, (f) desorption curves (g) velocity and (h) concentration terms of green plantain peels compared with the literature (Faneite *et al.*, 2012).

(89.1 %) resulted close to data reported in Monsalve *et al.* (2006). Raw protein content (8.81 %) was similar to data reported by Botero and Mazzeo (2009) despite of the variability caused by individual genomics, cultivar, altitude, climate, and ripening process (Mohapatra *et al.*, 2010). Crude fiber (5.13 %) and ash content (12.07 %) were coincident with data reported by Ly (2004) in an interval from 6.4 to 8.6% and 10.8 to 17.2 % respectively. Starch content (6.92 %) was found to be in the range 3-12.78 % reported by several authors (Wachirasiri *et al.*, 2009; Mohapatra *et al.*, 2010). Additionally, plantain peels were found to have a reduced amount of fat (2.47 %) and a high amount of NFE (71.55 %). The excellent nutritional value of plantain peels can be recognized by the high amount found of TDN (71.04 %). Finally, dry basis cellulose (6.68 %) and hemicellulose (45.40 %) was found to be high and lignin (2.93 %) found to be low. Compared with data reported in Faneite *et al.* (2012), plantain peels were found to have an HC content much higher than plantain leaves globally (29.16 %) or in the specific central vein of the leaf (21.46 %). Conversely, cellulose in plantain peels (6.68 %) was found to be lower than half the content

of the plantain leaves (15.47 %) and the fourth part of the content found in the central vein of the leaf (34.48 %) according to Faneite *et al.* (2012). Reported data could explain a slow drying behavior due to the high total content of carbohydrates, substances with a hydrophilic nature that could hinder the dehydration process.

Experimental drying plots at several temperatures for green plantain peels

Isothermal drying plots for green plantain peels in Figure 2a showed a monotonic decreasing for Mr in time in the whole range of temperatures studied, until the point where the changes of the weight were very little in function of the time, indicating that the transition state of dynamic pseudo-equilibrium (TSDPE) was reached. Further analysis about TSDPE was not considered due to the absence of interest from the economic point of view. Figure 2b showed a detail of the beginning of the TSDPE. The bigger value of the dynamic pseudo-equilibrium moisture was 2.80 % (w.b.) for the drying curve at 60 °C, decreasing with the increase of temperature. Taking into account, for example, the slope of the drying curve, in the TSDPE

Table 2. ANOVA and LSD of the statistical criteria of analytical selection

Model	R^2	MBE	MRD	RMSE	χ^2
modified Henderson and Pabis	0.9994 ^a	-9.77E-04 ^a	0.103 ^a	7.292E-03 ^b	5.929E-05 ^a
Midilli	0.9993 ^b	-1.23E-03 ^a	0.056 ^a	8.005E-03 ^a	7.066E-05 ^b

Superscripts “a” and “b” denote no significant difference between models with a 95 % confidence degree. R^2 : Coefficient of determination; MBE: Mean Biased Error; MRD: Mean Relative Deviation; RMSE: Root Mean Square Error; χ^2 : Chi square.

Table 3. Parameters of the modified Henderson and Pabis model

Temp. (°C)	<i>a</i>	<i>b</i>	<i>c</i>	<i>g</i> (x10 ³)	<i>h</i> (x10 ³)	<i>K</i> (x10 ³)
60	2.29	-1.01	-0.28	4.26	19.5	7.14
70	2.13	-0.87	-0.26	6.98	32.4	10.4
80	2.18	-0.91	-0.27	4.41	4.38	8.33
90	2.7	-1.54	-0.17	6.17	12.3	10.1
100	5.6	-3.03	-1.57	7.59	13.1	10.8
110	3.07	-2.02	-0.05	5.29	49.2	9.71

a, b, c, g, h and K are the parameters of the modified Henderson and Pabis model.

at 100 °C, of 0,000186251 kg H₂O/kg SS•min, and calculating an hypothetic real equilibrium moisture content using the equation proposed by Iguaz *et al.* (2003) for a similar lignocellulosic material. With the experimental conditions of this work, the real equilibrium moisture content would be reached in 4 hours 7 min, while the drying time was of 2 hours and half, from the initial moisture to the dynamic pseudo-equilibrium moisture content, not taking into account that the desorption of water could slow down in the extent that goes approaching to the real equilibrium. The difference between the static –real- and the dynamic pseudo equilibrium moisture content for this case is in an order of 10⁻², and any thin-layer drying empirical model, could reproduce this behavior.

Empirical modeling of drying plots for green plantain peels

In terms of visual inspection, behavior of experimental data was best suitably adjusted by means of the modified Henderson and Pabis model (Karathanos, 1999), and Midilli model (Midilli *et al.*, 2002). This can be observed in Figure 2a, where both models look almost identical. Table 2 show the statistical criteria employed to select the best data fitting to modified Henderson and Pabis (MHPM) and Midilli models (MM) in visual inspection. MHPM performed better following the “trend” of the experimental data. In terms of equitable distribution of the experimental points around the models (randomness), both models resulted in non-significant differences ($P < 0.05$). Finally, MM was the worst

in terms of the “bias” of the models with respect to the experimental points. Residuals of *Mr* for MHPM are shown in Figure 2c. This model reproduced optimally the experimental behavior in terms of random distribution of residuals and a bias of ± 0.025 of *Mr*. Table 3 shows the parameters of the selected model in the studied range of temperatures. Despite of having the same order, it could not be observed a clear trend correlating statistical parameters with temperature for any model.

Regular regime approach

Figure 2d show the potential pattern of the effective diffusivity in the whole range of *Mr* for all temperatures, confirming the concentration-dependence nature of the green plantain peels diffusivity. The increase of the effective diffusivity when decreasing *Mr*, may be due to the structural modification of the material while water is diffusing, increasing its porosity, as established by Weise (1998), leaving preferential ways to the most internal water, a behavior also seen in other polysaccharide materials (Saravacos, 2002).

Plotting *Deff* in function of *Mr* and *T* produced the equation 7, where, *Deff*:: effective diffusivity (m²/s), *T*: temperature (K), and *Mr*: remaining water fraction.

$$Deff = (-7,5621 \times 10^{-9} + 2,5158 \times 10^{-11} \times T) \times Mr^{-0,1726} \quad \text{Eq. 7}$$

Drying rate curves

Figure 2e shows that drying rate curves in the

range between 60 and 110 °C for green plantain peels, only had one period of decreasing drying with internal control. This was expected due to the natural barriers of the material avoiding desiccation and its hydrophilic polysaccharide matrix, whose crystallinity also changes with water desorption, thus agreeing with a concentration-dependence diffusional process nature (Weise, 1998). This behavior was observed in other lignocellulosic materials as lemna and cassava leaves (Medrano *et al.*, 2013; Suárez *et al.*, 2013). Any of the plots showed an adjusting initial period.

Desorption curves

Desorption isotherms of green plantain peels presented in Figure 2f show a sigmoidal shape in all cases, thus corresponding to a non Fickian or atypical diffusion pattern (Crank, 1975b), according with a concentration-dependence diffusional process, and with a drying with internal control. This result, was coherent with the observations of Faneite *et al.* (2012), for lemna, cassava leaves, corn leaves, sugar cane bagasse, sugar cane leaves, plantain leaves and midrib of plantain leaves, and by Suárez *et al.* (2013) for lemna.

Velocity term

Figure 2g shows the velocity term of plantain peels in the whole range of temperatures, accompanied by results of the application of regular regime approach to the desorption data of plantain leaves and midrib of plantain leaves available in the literature (Faneite *et al.*, 2012). Midrib of plantain leaves showed the highest velocity of drying. Probably this was due because this material is dedicated to the transport of fluids in the plant, and it is assumed that the water is diffused by the cuts and not through the midrib walls. When green plantain peels was separated from the vegetable, remained a face of the material that had no anti-dehydration barriers, with a high transference area with respect with the little cuts done to the plantain leaves. For this reasons it is assumed that plantain leaves have the slowest drying process.

Concentration term

Figure 2h shows the concentration term of green plantain peels compared with plantain leaves and midrib of plantain leaves (Faneite *et al.*, 2012). In order of ficktianity, plantain leaves drying are the most ficktian process followed by green plantain peels, being the midrib of plantain leaves the less ficktian process. This can be explained comparing the content of hydrophilic holocellulose (cellulose + hemicellulose) where the plantain leaves have the

less content (44.63 % in d.b.), followed by plantain peels (52.08 % d.b.), having midrib obviously the highest content (55.94 % d.b.), due to its character of supporting tissue.

Conclusions

A high proportion of carbohydrates and moisture level was found in fresh green plantain peels. Experimental drying plots showed a monotonic decreasing of the moisture content, followed by a transition state of dynamic pseudo-equilibrium where the changes in the moisture content are very small, and which begins in a moisture content under the traditional storage range (10–5 % in w.b.). Experimental drying plots were best fitted by the modified Henderson and Pabis model. Desorption, drying rate, and effective diffusivity curves showed a non ficktian process, a drying period of decreasing rate with internal control, and a concentration-dependence diffusion, respectively, demonstrating that the drying process of lignocellulosic materials is complex and computation of diffusion parameters should not be simplified without justification. The new terms associated with the regular regime approach proposal could explain the velocity of drying and the ficktianity of the process for lignocellulosic materials, in terms of the morphology of the samples and the hydrophilic compounds content as holocellulose, respectively.

Acknowledgement

Authors wish recognize Atencio family for their appreciated collaboration in the present work.

References

- Adhikari, B., Howes, T., Bhandari, B. R., Yamamoto, S. and Truong, V. 2002. Application of a simplified method based on regular regime approach to determine the effective moisture diffusivity of mixture of low molecular weight sugars and maltodextrin during desorption. *Journal of Food Engineering* 54(2): 157-165.
- Botero, J. D. and Mazzeo, M. H. 2009. Obtención de harina de ráquis del plátano dominico Hartón y evaluación de su calidad con fines de industrialización. *Vector* 4: 83-94.
- COVENIN. 1979. Norma 1156-79: Alimentos para animales. Determinación de humedad. Comisión Venezolana de Normas Industriales. Venezuela, Ministerio de Fomento. p. 11. Retrieved on September 22, 2011 from SENCAMER Website: <http://www.sencamer.gob.ve/sencamer/normas/1156-79.pdf>.
- COVENIN. 1981. Norma 376-81: Cacao y derivados. Determinación de almidón. Comisión Venezolana

- de Normas Industriales. Venezuela, Ministerio de Fomento. p. 4. Retrieved on September 22, 2011 from SENCAMER Website: <http://www.sencamer.gov.ve/sencamer/normas/1156-79.pdf>.
- Crank, J. 1975a. Diffusion in a plane sheet *The Mathematics of Diffusion*. 2nd edn. p. 50. Oxford: Clarendon Press.
- Crank, J. 1975b. Non-fickian diffusion *The Mathematics of Diffusion*. 2nd edn. p. 254-257. Oxford: Clarendon Press.
- Chambron, A. C. 2000. Straightening the bent world of the banana. Report of the European Fair Trade Association. Brussels: EFTA.
- Espinosa, J. and Mite, F. 2002. Estado actual y futuro de la nutrición y fertilización del banano. *Informaciones Agronómicas (INPOFOS)* 48: 4-10.
- Faneite, A., Ferrer, A., Aiello-Mazzarri, C., Villegas, J. and Gnansounou, E. 2012. Interaction Between Chemical Composition, Microcrystalline Structure and Morphology of the Most Important Agricultural Byproducts in the Northern of South America, and its Drying Kinetic. In: Chiaramonti, D., and Raina, V.N. (Eds). *Proceeding of the XIX International Symposium on Alcohol Fuels (ISAF)*, p. 439-442. Verona: University of Florence. ISBN 978-88-7743-369-5.
- FAO. 2013. Estadísticas de la Organización de las Naciones Unidas para la Agricultura y la Alimentación. Retrieved on December 03, 2013 from FAO Website: <http://faostat.fao.org/site/339/default.aspx>.
- Garrett, W. N. 1974. Estimation of the Nutritional Value of feeds. In: Cole, H. H., and Garrett, W. N. (Eds.), *Animal agriculture*, p. 501-514. Washington: Freeman and Company.
- Iguaz, A., Esnoz, A., Martínez, G., López, A. and Virseda, P. 2003. Mathematical modelling and simulation for the drying process of vegetable wholesale by-products in a rotary dryer. *Journal of Food Engineering* 59(2): 151-160.
- Intriago, F. and Paz, S. 2000. Ensilaje de cáscara de banano maduro con microorganismos eficaces como alternativa de suplemento para ganado bovino. Guácimo, Costa Rica: Universidad Earth, Bachelor Thesis.
- Karathanos, V. 1999. Determination of water content of dried fruits by drying kinetics. *Journal of Food Engineering* 39: 337-344.
- Ly, J. 2004. Bananas y plátanos para alimentar cerdos: aspectos de la composición química de las frutas y de su palatabilidad. *Revista Computarizada de Producción Porcina* 11(3): 5-24.
- Medrano, J., Rondón, K., Faneite, A. and Ferrer, A. 2013. Modelado del secado en capa fina de las hojas de yuca. In: Muñoz C., D. (Ed). *Proceeding of the II Congreso Venezolano and III Jornadas Nacionales de Investigación Estudiantil "Dra. Luz Maritza Reyes"*, p. 378-396. Maracaibo: Universidad del Zulia.
- Midilli A., Kucuk H. and Yapar Z. 2002. A new model for single layer drying. *Drying Technology* 20(7): 1503-1513.
- Mohapatra, D., Mishra, S. and Sutar, N. 2010. Banana and its by-products utilization: an overview. *Journal of Scientific and Industrial Research* 69, 323-329.
- Molnár, K. 2006. Experimental Techniques in Drying. In: A. S. Mujumdar (Ed.), *Handbook of industrial drying*. 3rd edn. p. 39-40. Boca Ratón: CRC Press.
- Monsalve, J., Medina, V. and Ruiz, A. 2006. Producción de etanol a partir de la cáscara de banano y de almidón de yuca. *Dyna* 73(150): 21-27.
- OPEC. 2015. Annual Statistical Bulletin. Organization of the Petroleum Exporting Countries. Retrieved on October 13, 2013 from OPEC Website: http://www.opec.org/opec_web/en/publications/202.htm.
- Rao, M. A., Rizvi, S. S., Datta, A. K. and Ahmed, J. 2014. *Engineering properties of foods*. 4th edn. p. 315-321. New York: CRC Press.
- Saravacos, G. D. 2002. Transport Properties in Food Engineering. In: Welti-Chanes, J., Barbosa-Cánovas, G. V., and Aguilera, J. M. (Eds). *Engineering and Food for the 21st Century*, p. 188. Boca Ratón: CRC Press.
- Suárez, L., Faneite, A. and Ferrer, A. 2013. Modelado del secado en capa fina y del presecado al sol a distintas condiciones de la Lemna obscura del lago de Maracaibo. *Revista Tecnocientífica Universidad Rafael Urdaneta* 4: 75-85.
- Treybal, R. 1980. Operaciones de transferencia de masa. 2nd edn in Spanish. p. 747-750. New York: McGraw-Hill Book Co.
- Van Soest, J. 1963. Use of detergents in the analysis of fibrous feeds. II. A rapid method for determination of fiber and lignin. *Journal of the Association of Official Agricultural Chemist* 46: 829-834.
- Wachirasiri, P., Julakarangka, S. and Wanlapa, S. 2009. The effects of banana peel preparations on the properties of banana peel dietary fibre concentrate. *Songklanakarin Journal of Science and Technology* 31(6): 605-611.
- Weise, U. 1998. Hornification - mechanism and terminology. *Paperi ja puu - Paper and Timber* 80(2): 110-114.